THE BALTIC JOURNAL
OF ROAD AND BRIDGE ENGINEERING

ISSN 1822-427X / eISSN 1822-4288
2017 Volume 12(3): 145–153

STATISTICAL-NUMERICAL ANALYSIS FOR PULLOUT TESTS OF GROUND ANCHORS

Juraj Chalmovský[1], Jan Štefaňák[2], Lumír Miča[3], Zdenek Kala[4], Šarūnas Skuodis[5]✉, Arnoldas Norkus[6], Daiva Žilionienė[7]

[1, 2, 3]*Dept of Geotechnics, Brno University of Technology, Veveří 331/95, 602 00 Brno, Czech Republic*
[4]*Institute of Structural Mechanics, Brno University of Technology, Veveří 331/95, 602 00 Brno, Czech Republic*
[5]*Dept of Geotechnical Engineering, Vilnius Gediminas Technical University, Saulėtekio al. 11, Vilnius 10223, Lithuania*
[6]*Geotechnical Research Laboratory, Vilnius Gediminas Technical University, Saulėtekio al. 11, Vilnius 10223, Lithuania*
[7]*Dept of Roads, Vilnius Gediminas Technical University, Saulėtekio al. 11, Vilnius 10223, Lithuania*
E-mails:[1]*chalmovsky.j@fce.vutbr.cz;* [2]*stefanak.j@fce.vutbr.cz;* [3]*mica.l@fce.vutbr.cz;* [4]*kala.z@fce.vutbr.cz;*
[5]*sarunas.skuodis@vgtu.lt;* [6]*arnoldas.norkus@vgtu.lt;* [7]*daiva.zilioniene@vgtu.lt*

Abstract. The paper presents an application of statistical and numerical methods for the determination of the force-displacement curves and that of pullout capacity of prestressed grouted ground anchors installed in Miocene clay. A regression analysis of data from a database of acceptance test records for ground anchors to create has been performed, the force-displacement curve of the tested anchor corresponding to the range of loads applied for acceptance tests has been created. A linear regression model, employing the weighted least squares method and robust standard errors techniques were concluded to serve as a reliable statistical method suitable for achieving this goal. The discovered linear regression dependence then served as a lower control limit for the displacement values calculated at the anchor head applying the numerical model. A finite element model has been created to predict the behaviour of ground anchors being installed in fine-grained soils. The developed numerical model that employs Mohr-Coulomb strength criterion constitutive model evaluates the influence of high-pressure grouting by development additional radial stresses and that of an increment of fixed length diameter.

Keywords: Finite Element Method (FEM), ground anchor displacement, high-pressure grouting, numerical analysis, statistical analysis.

1. Introduction

The pressure grouting is found to be one of the most significant factors determining pullout capacity of ground anchors. Domes (2015) investigated the influence of pressure grouting in the non-cohesive soil. The impact of pressure grouting on the stress magnitudes on the anchor surface and the properties of the adjacent soil have been studied. Lee *et al.* (2012) analysed the influence of pressure grouting on the diameter enlargement and the pullout force of compression ground anchors. Post-grouting has been experimentally investigated by e.g. Littlejohn (1980) and Jones *et al.* (1980). Mišove (1984) carried out an extensive testing program on ground anchors, including excavation and detailed examination of fixed length shapes and their increased diameters. Mecsi (1997) analysed radial stress acts on the surface of the fixed length of the anchor in detail.

This process is possible to modelling by numerical methods. Desai *et al.* (1986) analysed the interaction of a ground anchor with surrounding soil by using a 3D mathematical model and the Finite Element Method (FEM). Kim *et al.* (2007) investigated a load transfer mechanism from a prestressed ground anchor to sandy clay by using the ABAQUS software. Tchuchnigg (2008), Ghosh and Kumar (2015) also applied FEM techniques for ground anchor behaviour analysis. Hu and Hsu (2012) applied FLAC software to simulate the anchor-soil interaction of load tests.

The anchor pullout capacity determined by the FEM needs to be validated by investigation tests. The number of investigation tests currently is very limited in the practice Duzceer *et al.* (2015), Ene *et al.* (2014), Jacquar Fondasol (2014). However, there is the relatively large amount of data available from acceptance tests (due to the requirements of standards for prestressed soil anchors, e.g. *EN 1537 Execution of Special Geotechnical Work - Ground Anchors* in Europe or *PTI DC35.1-14: Recommendations for Prestressed*

doi:10.3846/bjrbe.2017.17

Rock and Soil Anchors in the US, an acceptance test must be carried out on every system anchor).

Statistical analyses for measured pullout resistances have been conducted previously following procedures by Hegazy (2002). The correlation the forces of applied traction versus the corresponding measured elongations of ground anchor tendon was analysed by Sciacca *et al.* (2014). Shahn (2014) used the evolutionary polynomial techniques to model the pullout capacity of small ground anchors.

Hence, the authors decided to perform statistical analysis procedures with available test data and subsequently employ the obtained results as an alternative means of checking the FEM model. The combination of statistical method and FEM, including post-grouting effect, for the determining of the force-displacement curve and that of the pullout capacity of prestressed grouted ground anchors is applied in the investigation.

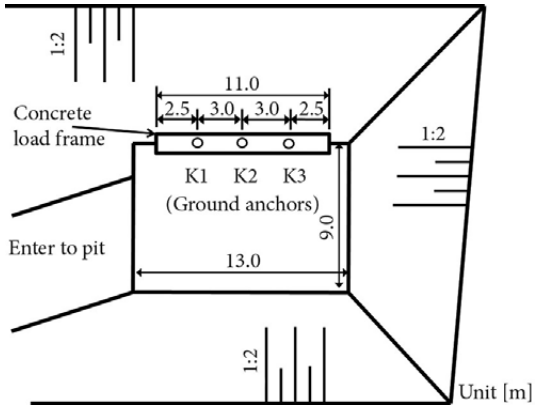

Fig. 1. Schematic ground plan of the test site

Table 1. Tested anchor description

Characteristic of anchor	Investigation tests	Acceptance tests
Type of anchor*	Temporary $8\times L_p$15.7–1770	Temporary $8\times L_p$15.7–1770
Free anchor length L_{free}	8.1 m	11.0 m
Fixed anchor length L_{fixed}	11.5 m	11.5 m
Inclination of the borehole	63.5°	22°

Note: * the tendon consists of eight cables with a diameter of 15.7 mm and a tensile strength of 1770 MPa.

Table 2. Properties of Miocene clay

Properties	Symbol	Unit	Value
Water content	w	%	30.6
Liquid limit	w_L	%	62.0
Plasticity limit	w_P	%	24.5
Particle density	ρ_s	kg·m^{-3}	2692
Void ratio	e	–	0.67

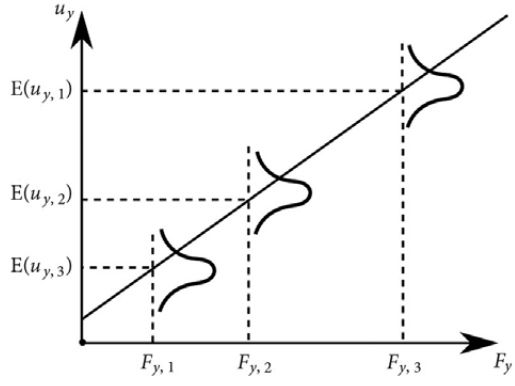

Fig. 2. Schematics of the stochastic dependence anchor head displacement versus proof load

2. Field load test

Full-scale anchor pullout load tests (ULS) have been performed for three high-pressure grouted anchors in the experimental site in Czech Republic (Fig. 1) before the construction of a railway tunnel have been started by Velič, Mišove (2004). Tests were equipped for determining maximum pullout forces magnitudes (Fig. 1). The results from this type of test have been employed for back-analysis procedures. Sixty eight system anchors have been then used for supporting a diaphragm wall during the construction of a tunnel. The acceptance tests were set up via the same technical procedures and in the same geological conditions as those employed in the investigation tests. The characteristics of the tested anchors are summarized in Table 1.

The ground anchors have been installed in Miocene clay with very high, locally extreme, plasticity (symbol CV and CE according to the USCS). The clay was fully saturated. The index properties of Miocene clay are summarized in Table 2.

3. Construction of the stress-strain diagrams of anchors from acceptance test data using regression analysis

Acceptance test reports of sixty eight above mentioned system anchors have been created during the loading according to *EN 1537: 2001*. The displacement u_y and the force F_y (proof load) at the anchor head have been measured at each loading cycle. The relationship between these two variables is described via stochastic dependence, that takes multiple u_y values derived from a specific probability distribution for one particular F_y value (Fig. 2). The aims of the regression analysis are:

(i) to find the parameters of the linear relation of variables *uy* versus F_y and

(ii) to confirm the correctness and assumptions of the linear regression model.

One of the assumptions of linear regression model states that the mean values E($u_{y,1}$), E($u_{y,2}$), E($u_{y,3}$) lie on the line. The mean values E($u_{y,i}$) are the means of probability distributions of the displacement u_y. Samples of u_y come from measurement of displacement at a specific level of the force F_y for every system anchor. Assessment procedures resulted that the dependence the proof load versus displacement (measured at the anchor head) is almost linear. Assumptions of the linear regression model are:

1) it is adopted a specified model, equation is correctly selected;

Table 3. Probability distribution parameters of measured displacements for the particular stressing force level

Stressing force level, kN	Probability distribution	Mean, mm	Standard deviation, mm	Variation coefficient	Skewness	Kurtosis
444	Bradford	21.358	3.980	0.186	0.261	–1.023
777	Beta	41.074	4.468	0.114	–0.026	–0.406
1110	GumbelMin. EV I	64.627	5.648	0.087	–0.589	0.026

2) mean error term is equal to zero;

3) an error has a constant variance component (Homoscedasticity condition);

4) the components of the error vector are uncorrelated;

5) the residual component has a normal distribution.

Verification of these assumptions is carried out further in Sections 3.1–3.8. GRETL software has performed regression analysis. The chosen significance level of all tests was $\alpha = 0.05$.

3.1. Measured data analysis

The data report results of acceptance tests have been employed as the input data for the regression analysis. The displacements have been measured for each anchor for three load levels. Following the Anderson–Darling Goodness-of-Fit test (Anderson, Darling 1952, 1954), the appropriate probability distribution is allocated to the displacement data set measured at each load level (Table 3).

For comparison, the stress-strain diagrams of the system anchors have been adjusted for elastic strains (corresponding to the free length difference of both anchor types (Table 1)).

3.2. Model quality evaluation

An estimation of regression parameters β_i has been performed applying the least squares method (LSM). Subsequently, the regression diagnostic has been done. It included checking the LSM assumptions and evaluating the quality of the β_i coefficients. The following Eq summarizes the obtained final result:

$$u_y = -6.28 + 0.05F_y\,. \tag{1}$$

A graph of the determined regression model is plotted in Fig. 3.

One must note, that an application of the linear regression model includes several additional assumptions, which should always be verified using appropriate diagnostic methods.

3.3. Variance analysis

The variance analysis (ANOVA) has been carried out for quantifying the variability of the created regression model. The residual sum of squares (RSS) and the determination coefficient R^2 were calculated via this analysis.

The Pearson correlation coefficient R and the standard error of the regression $\hat{\sigma}$ were also quantified. The data of variance analysis results of the linear regression model are presented in Table 5.

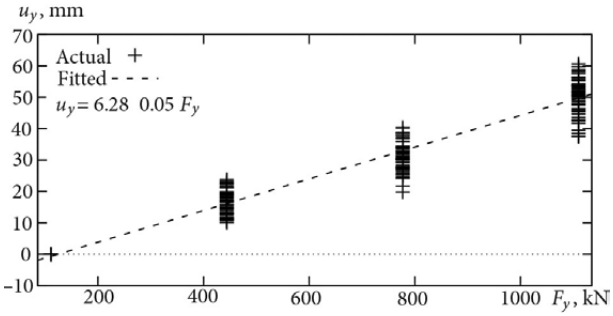

Fig. 3. Linear regression model built using least squares method

3.4. Confidence interval for regression coefficient

The *p*-value of the *t*-statistics, calculated for the βi coefficients indicates the maximal possible level of trust for which the null hypothesis *H0*: $\beta_i = 0$ is acceptable. Confidence intervals with 95% probability have been constructed for both parameters (Table 5). The confidence ellipse serves as point estimate of the regression parameters (Fig. 6).

3.5. Testing of LSM assumptions

There are some assumptions behind the LSM:

- regression coefficients βi can take arbitrary magnitudes,
- the regression coefficients are linear, the additive model of measuring is valid.

There is an assumption for the vector of residuals ε, stating that its elements are independent. The verification of linear regression (1) includes verification of normality of the value ε. They correspond a normal distribution with null mean and finite variance $E(\varepsilon^2) = \sigma^2$ (homoscedasticity) (Meloun, Militký 2011).

3.6. Heteroscedasticity testing

Heteroscedasticity term states that variance is parameter-dependent. The White and Breusch–Pagan (Yurekli, Kurunc 2005) tests of null hypothesis *H*0: *checking if data are homoscedastic* were carried out. The summarized results of those tests are presented in Table 4. In analysed case the processed data result in heteroscedasticity. Subsequently, the LSM analysis requires modification procedures for the next step. It is evident also from Fig. 4 that the variance in the analysed case is variable for all data.

3.7. Testing the normality of the error distribution

The assumption of the standard distribution of errors introduces the null hypothesis *H0: the vector of errors is usually distributed and has null mean value*. If the distribution is normal, the points on normal quantile plots of the

residuals *Q*-*Q* fall close to the diagonal reference line $y = x$. The *S*-shaped pattern of deviations indicates excessive kurtosis of residuals (Fig. 6).

The *Chi*-square Goodness-of-Fit test (Pearson 1900) with the final *p*-value = 0.075 has been carried out for verification of the error distribution normality. Because of the trial, one can state that the normality of the error

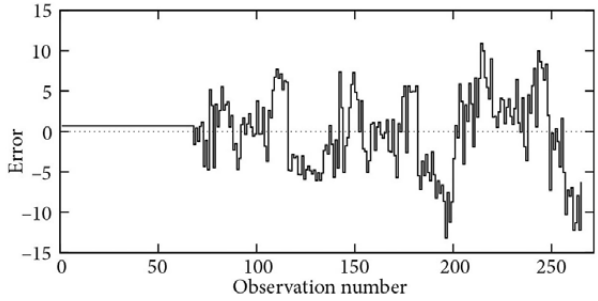

Fig. 4. Graph of residuals by observation number

Table 4. Results of the heteroscedasticity tests

Heteroscedasticity Test	Test statistic value	*p*-value
White	47.754	4.269e–011
Breusch-Pagan	55.783	8.092e–014

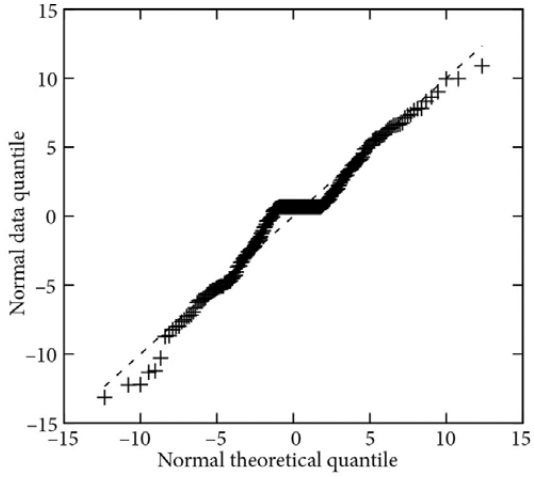

Fig. 5. Graph of residuals by observation number

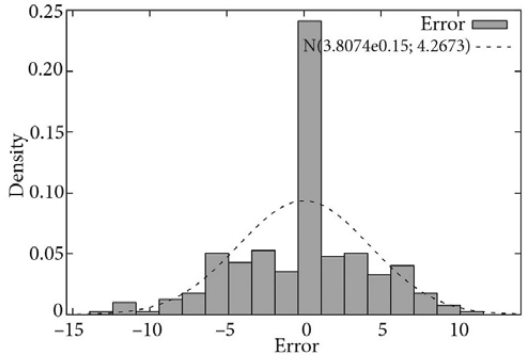

Fig. 6. Histogram of standard errors (graphical presentation of the *Chi*-square Goodness-of-Fit test)

assumption of the considered linear regression model is valid. Figure 6 presents the graphical output of the *Chi*-square Goodness-of-Fit test (the skewness of the distribution of residuals is 0.173, and the kurtosis is 0.311).

3.8. Weighted Least Squares Method

It is possible to correct the estimates of the β_i coefficients of the model by using the weighted least squares method (WLSM). Instead of finding the minimum of the function

$$RSS = \sum_{1}^{n} \left(y_i - \left(\beta_1 + \beta_2 x_i \right) \right)^2 , \tag{2}$$

the minimum weighted sum of squared residuals

$$RSS_w = \sum_{1}^{n} w_i \left(y_i - \left(\beta_1 + \beta_2 x_i \right) \right)^2 \tag{3}$$

is determined. The latter gives more efficient estimation of β_i coefficients. Here w_i is a non-negative constant, referred to as weight. The weight was determined using the heteroscedasticity-corrected linear regression model. Equation (4) defines weight w_i :

$$w_i = \frac{1}{e^{(u^*)}}, \tag{4}$$

where u^* are output values, obtained from the auxiliary regression function considering the dependence of quadrate logarithms of residuum (from the model constructed using the LSM) and interpreting the variable x_i and its quadrate magnitudes

$$\log \varepsilon^2 = \beta_{1,aux} + \beta_{2,aux} x_i + \beta_{3,aux} x_i^2 + \varepsilon_{aux} . \tag{5}$$

3.9. Summary of the regression analysis and discussion of results

Two model variants describing the dependence of u_y versus F_y have been developed, following the procedures described above:

$$\text{LSM: } u_y = -6.28292 + 0.0504999 F_y + \varepsilon , \tag{6}$$

$$\text{WLSM: } u_y = -5.58890 + 0.0496875 F_y + \varepsilon . \tag{7}$$

It was found that the WLSM yields higher accuracy dependence of u_y versus F_y comparing with the one obtained by LSM having performed the regression diagnostic. The *p*-values of the β_i coefficients are lower the ones obtained by the WLSM. The confidence intervals of the β_i coefficients are narrower for WLSM (Table 6, Figs 7 and 8). The determined residual sum of squares RSS and Akaike Information Criterion (AIC) values are less in the case of the second model. The higher R^2 indicates the higher explanatory power of the WLSM (Table 5).

Table 5. Quality comparison of estimated models

Model	RSS	*F*	*p*-value *F*	R^2	*R*	$\hat{\sigma}$	AIC
LSM	4789	5159	7.6e–175	0.9515	0.975	4.26	1523
WLSM	628	10161	3.5e–212	0.9748	0.9873	1.55	984

A branch of the stress-strain diagram for the anchor is constructed as a base for the regression model (7) and is plotted in Fig. 11.

The verification analysis of the assumptions of linear regression model confirmed the linear dependence of the proof load versus displacement. The correctness of the specified model and him assumptions of mean error term equal to zero have been met. The hypothesis of the normal distribution of residual components is also valid. The assumptions of the constant error of variance component was not met, which led to an adjustment of the LSM. The obtained results are valid for the loading intervals of performed acceptance tests.

4. Finite element analysis

The Plaxis software 2D (Brinkgreve *et al.* 2012) have been employed for numerical (FEM) modelling of the pullout resistance for ground anchor. An axisymmetric model, a width of 12 m and a height of 24 m has been created. The anchor has been modelled vertically positioned to achieve the condition of axisymmetry. The latter is a certain simplification compared with reality (Table 1).

4.1. Description of the 2D mathematical model

The mesh of 2D 15-nodded triangular finite elements with fourth order interpolation of displacement and twelve Gauss points for the numerical integration have been employed along anchor length. An additional mesh refinement has been set close to the fixed length of the anchor (Fig. 10). Figure 10a presents meshes (optimized and initial) and Fig. 10b the transition from the free to the fixed length. Displacement controlled loading at the anchor head has been adopted. The interface anchor body and surrounding soil have been modelled by the interface of finite elements, which is implemented in software Plaxis.

The total influence of post-grouting is done by two aspects:

(i) increasing of diameter of the fixed body of the anchor,

(ii) increasing of a radial stress caused by its volumetric expansion due to the post-grouting.

Prescribed volumetric strain values of the relevant finite elements have been assigned to introduce the effect of the post-grouting (Fig. 9).

Similar procedures have been applied in, e.g. for the mathematical modelling of compensation grouting (Kummerer 2003). The volume of elements change ΔV_0^e is a function of the given volumetric strain and that of the original volume V_0^e:

$$\Delta V_0^e = \varepsilon_{T,vol} V_0^e . \quad (8)$$

Table 6. Confidence intervals of the parameters for the LSM

Model	Coefficient	*p*-value	95% confidence interval	
LSM	β_1–const	1.59e–028	–7.2709700	–5.2948600
	β_2–F_y	7.56e–175	0.0491156	0.0518843
WLSM	β_1–const	3.30e–099	–5.9092800	–5.2685300
	β_2–F_y	3.52e–212	0.0487170	0.0506581

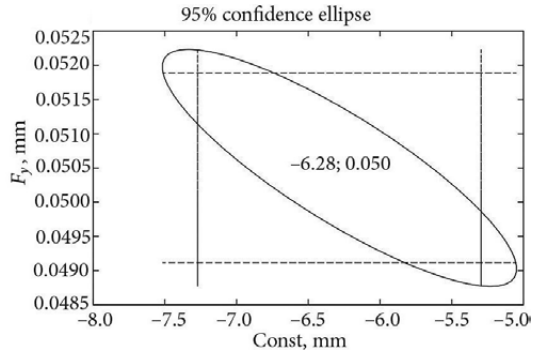

Fig. 7. Confidence ellipse of regression coefficients for the LSM

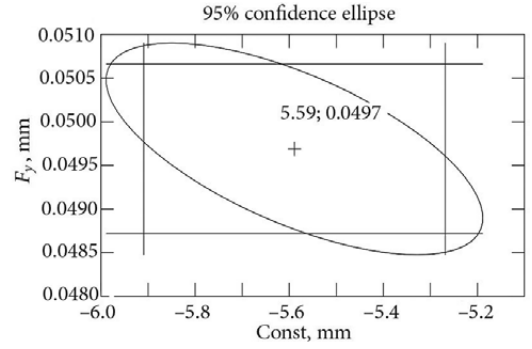

Fig. 8. Confidence ellipse of regression coefficients for the WLSM

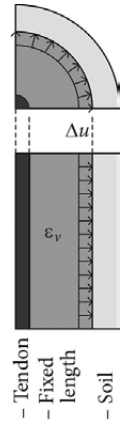

Fig. 9. Consideration of high-pressure grouting in the Finite Element Model

The components of the volumetric strain vector $\underline{\varepsilon_t}$ are as follow (in the case of the isotropic volumetric strain):

$$\underline{\varepsilon_t} = \left\{\varepsilon_{T,xx};\ \varepsilon_{T,yy};\ \varepsilon_{T,zz};\ \varepsilon_{T,xy};\ \varepsilon_{T,yz};\ \varepsilon_{T,zx}\right\}^T, \quad (9)$$

$$\varepsilon_{T,xx} = \varepsilon_{T,yy} = \varepsilon_{T,zz} = \frac{\varepsilon_{T,vol}}{3}, \quad (10)$$

$$\varepsilon_{T,xy} = \varepsilon_{T,yz} = \varepsilon_{T,zx} = 0. \quad (11)$$

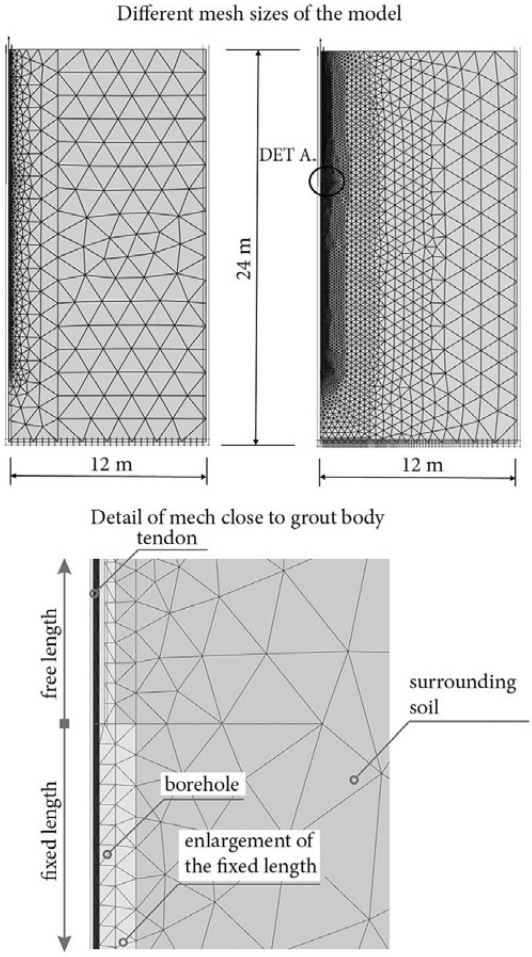

Fig. 10. Finite element mesh of model

Table 7. Input parameter values for the M-C model

Input parameter			Value
Name	Symbol	Unit	
Unit weight	γ	kN/m^3	20.5
Young's modulus	E_{ref}	kPa	5000
Puasson's coef.	ν_{ref}	–	0.3
Cohession	c'_{ref}	kN/m^2	8.0
Angle of internal friction	φ'	°	0
Shaft friction coef.	R_{inter}	–	1.0

The Mohr-Coulomb (M-C) model was chosen for simulation of soil behaviour Brinkgreve *et al.* (2012). Input parameters have been determined for the available geological survey; relevant technical reports have been produced by company Amberg Engineering Brno a.s. (Table 7).

During the loading of a grouted ground anchor, the grout in the fixed length have been stressed by gradual tension up to the tensile strength limit magnitude. Tensile cracks occurred during the process. When using the linear elastic model, the tensile stress magnitude is unlimited. Due to the M-C model, tensile stress limitation has also been applied to the grout material. An additional plasticity function is available (Eq 12), where is the maximum allowable tensile stress (tensile strength) magnitude. The grouting material has strength in tension σ_t = 2000 kPa, so:

$$f_t = \sigma'_1 - \sigma_t. \quad (12)$$

4.2. Methodology of the performed analysis

According to Mišove (1984), the grouted ground anchor final diameter of anchor root varies within the range of 20 cm to 40 cm, depending on geological conditions. By this assumption, one can determine the available values of the volumetric strains, that serve as input data for the calculation procedures. A parametric study has been performed to investigate the influence of the diameter, which varied within the interval mentioned above range (Table 8, steps 2a, 2b, and 2c). In the final step 3 (Table 8), the increase in the diameter of the fixed length of the anchor (d_{fixed} = 40 cm) has been considered in combination with neglecting the corresponding volumetric strain being induced actually. By combining the separate initial data, one can investigate the relative influence of both factors (of diameter and that of radial stress) for anchor behaviour. The performed modelling cases are presented in Table 8.

Table 8. Methodology of the performed analysis

ID	d_{fixed}, mm	Volumetric strain	Description
1	156	No	Only gravity (tremie) grouted
2a	200	Yes	Calculation with anchor root diameter expansion to d = 20 cm with corresponding volumetric strain
2b	300	Yes	Calculation with anchor root diameter expansion to d = 30 cm with corresponding volumetric strain
2c	400	Yes	Calculation with anchor root diameter expansion to d = 40 cm with corresponding volumetric strain
3	400	No	Calculation with anchor root diameter expansion to d = 40 cm without the inclusion of corresponding volumetric strain

4.3. Summary of the FEM analysis and discussion of results

Force versus deformation diagrams has been plotted for each case (Figs 11 and 12). Besides the FEM calculation results, the regression dependence found using the WLSM (Chapter 3) and the measurements from three investigation load tests (anchors K1 to K3) have been added to Figs 12 and 13.

The alternative analysis case ID 1, which ignores the post-grouting influence, significantly underestimates the anchor pullout capacity. In the case ID 2a, the theoretical pullout capacity has been reached prematurely. For case ID 2b a better prediction has been obtained comparing with that of for ID 2a case, though the calculated pullout capacity was still lower than the measured capacity by experiments one. For the last considered alternative ID 2c, the satisfactory agreement of measured versus computed displacements has been reached even at the highest load increment stages. One must emphasize that final state has been not reached during the investigation test despite a substantial increase in anchor permanent displacements. The latter situation conforms to the ID 2c prediction. The linear regression provides a sufficient match with the measured and computed displacements for several first loading stages (lower than 500 kN magnitude). For larger load magnitude stages, the regression analysis underestimates the anchor head displacement. The latter finding confirms the significant contribution of permanent soil plastic deformations developed on the soil – anchor interface.

The limit state in case ID 3 has been achieved foremost comparing with remaining simulation cases (Fig. 12); the calculated ultimate (pullout) force magnitude was even lowered the one determined by ID 2b one. The larger computed ultimate force magnitude has been obtained for the case ID 2c. In this case, the factor of effective radial stress increment, and consequently, the shear strength increment has been taken into account. The distributions of the mobilized shear stress and the radial stress in the horizontal cut at the middle of the fixed length for the final stage are presented in Fig. 13.

Mobilised relative shear stress distribution around the fixed anchor length that of for vertical displacement are plotted for case ID 2c (Fig. 14).

5. Conclusions

The paper summarized a set of pullout testing data for ground anchors in concern with performed numerical simulations of appropriate behaviour. Comparative analysis of testing and simulation results yield proper linear response for anchor soil base versus applied load. The paper focused on the prediction of force-displacement curves, rather than on the determination of the pullout capacity of ground anchors. Depending on the results of this study, the following conclusions are drawn:

1. Statistical analysis – the process of constructing the force-displacement curves of anchors from a set of acceptance tests via the use of the Weighted Least Square Method

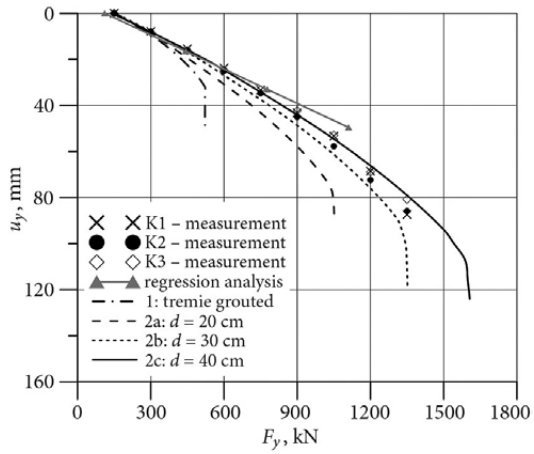

Fig. 11. Comparison of the results of investigation load tests, regression analysis, and numerical analysis

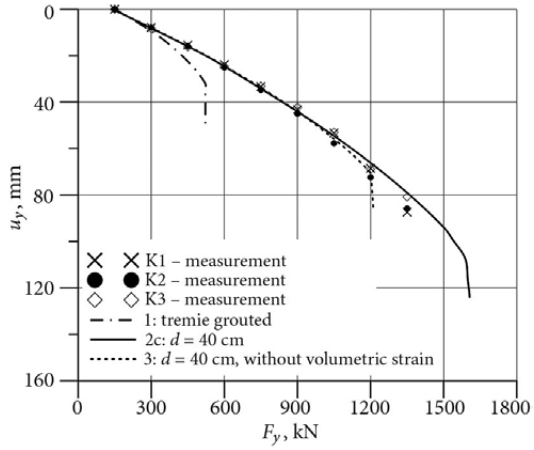

Fig. 12. Influence of the applied volumetric strain

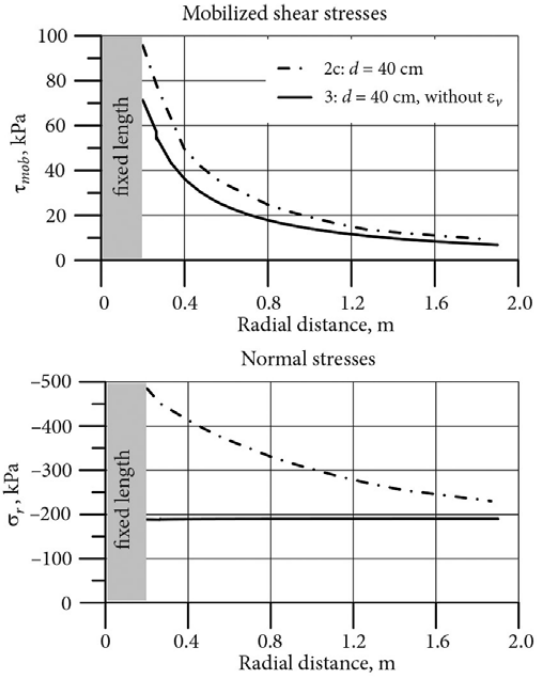

Fig. 13. Distribution of stresses in the horizontal (radial) direction

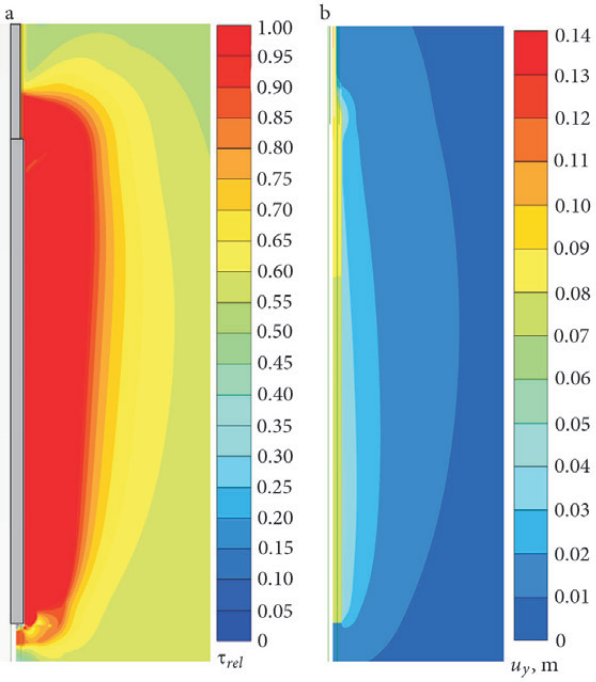

Fig. 14. Distribution of the relative shear stresses (a) and vertical displacement (b)

with an appropriately chosen weighted coefficient is described. The Weighted Least Square Method has been selected as the optimal method for this investigation via the regression diagnostic (of the qualitative evaluating criteria for two alternative models). When compared to the curve from the investigation test, the statistically determined force-displacement curve diverges from the certain prestressing force value. This result has been obtained despite the fact that determination coefficient magnitudes are large. The following result is conditioned by an application of the linear trend in the Weighted Least Square Method, regression model. This model is unconcerned with the nonlinear strain increase at the anchor bond (the permanent/plastic part of the displacement). The use of the linear trend is nevertheless justified because the force-displacement curve is almost linear in the range of considered load variation bounds, which are usually applied for acceptance tests. The importance of the constructed linear regression dependence lies in the determination of the lower control limit of the displacement values at the anchor head for the evaluation of the developed numerical model.

2. Numerical analysis – the Finite Element Method techniques have been employed to predict the force-displacement behaviour of the grouted ground anchor. The Finite Element Method analysis focused on considering the impact of high-pressure grouting. Soil-structure interaction has been simulated by using zero thickness interface elements. The Mohr-Coulomb constitutive model has been employed both for the surrounding soil and of the grout material with the aim to limit grout tensile strength.

The final analysis using the Finite Element Method proved that high-pressure grouting is the significant influence predetermining behaviour of the anchor (both on the shape of the force-displacement curve and the ultimate carrying capacity). Five different analysis cases have been performed. The high-pressure grouting has been simulated via an increasing the diameter of the ground anchor body and by the additional application of volumetric strain to the relevant finite elements. The best fit has been reached for the simulation with a diameter expansion to 40 cm and with the corresponding volumetric strain development. The reasonable match has been achieved when comparing the force-displacement curves of the ground anchor, constructed by using the mathematical model described above and the load-displacement curve obtained from the investigation tests.

The presented study confirmed that considering the influence of high-pressure grouting via the Finite Element Method techniques and the combination of the diameter increment for the fixed length of the anchor and that of the corresponding volumetric strain introduction ensures the important increase of accuracy for prediction of the load-displacement curve and subsequently for determining the proper ultimate pullout capacity magnitude.

One must emphasize that these proposed models have been used for the particular type of anchors, similar to analysed in paper ones, namely: prestressed grouted ground anchors with steel strand tendon placed in clays of very high plasticity. The latter limitation is conditioned by the fact that relative anchor-soil stiffness significantly influences the behaviour of structures like ground anchors. For different as to analysed conditions, namely for various type of pressure grouting, confining stress, soil type, and anchor type, the developed analysis models, have to be appropriately adjusted.

Acknowledgements

This research was financially supported by the Ministry of Industry and Trade of the Czech Republic under research project No. FR-TI4/329 and Centrum AdMaS "Advanced Materials, Structures, and Technologies" Regional Centre (grant No. CZ.1.05/2.1.00/03.0097). The authors thank the companies Amberg Engineering, VUIS-Zakladanie Stavieb, s.r.o. and SŽDC for providing the documentation.

References

Anderson, T. W.; Darling, D. A. 1952. Asymptotic Theory of Certain "Goodness of-Fit" Criteria Based on Stochastic Processes, *Annals of Mathematical Statistics* 23(2): 193–212. https://doi.org/10.1214/aoms/1177729437

Anderson, T. W.; Darling, D. A. 1954. A Test of Goodness-of-Fit, *Journal of the American Statistical Association* 49(268): 765–769. https://doi.org/10.1080/01621459.1954.10501232

Desai, C.; Muqtadir, A.; Scheele, F. 1986. Interaction Analysis of Anchor-Soil Systems, *Journal of Geotechnical Engineering* 112(5): 537–553. https://doi.org/10.1061/(ASCE)0733-9410(1986)112:5(537)

Domes, X. A. 2015. *Cement Grouting during Installation of Ground Anchors in Non-Cohesive Soils.* PhD thesis. Trondheim, Norwegian University of Science and Technology.

Duzceer, R.; Mothersille, D.; Okumusoglu, B.; Gokalp, A. 2015. Support of 25 m Deep Excavation Using Ground Anchors in Russia, in *Proc. of the ICE – Geotechnical Engineering*. 168(4): 281–295. https://doi.org/10.1680/geng.14.00043

Ene, A.; Marcu, D.; Popa, H. 2014. Testing of Ground Anchorages for a Deep Excavation Retaining System in Bucharest, in *Proc. XV Danube – European Conference on Geotechnical Engineering (DECGE 2014),* 9–11 September 2014, Vienna, Austria, Paper No. 176. 6 p.

Ghosh, P.; Kumar, R. 2015. Numerical Study on Static Interaction of Closely Spaced Horizontal Square or Rectangular Ground Anchors in *c-ϕ* Soil, *International Journal of Geosynthetics and Ground Engineering* 1(4):1–7. https://doi.org/10.1007/s40891-015-0037-z

Hegazy, Y. A. 2002. Reliability of Estimated Anchor Pullout Resistance, *Grouting and Ground Treatment*. Reston, VA: American Society of Civil Engineers, 772–779.

Hu, W. C.; Hsu, S. T. 2012. Numerical Modelingof Earth Structures: Frictional Anchors in Sand, *Advanced Materials Research* (486): 214–220. https://doi.org/10.4028/www.scientific.net/AMR.486.214

Jacquar Fondasol, F. C. 2014. Foundations by Prestressing Anchors of the "Villa Méditerranée" in Marseille from Design to Monitoring, in *Proc. of the ISSMGE Technical Committee 207 International Conference on Geotechnical Engineering – Soil-Structure Interaction, Underground Structures and Retaining Walls*, 16–18 June 2014, St Petersburg, Russia. 127–131. http://doi.org/10.3233/978-1-61499-464-0-127

Jones, D. A.; Turner, M. J. 1980. Load Tests on Post-Grouted Micropiles in London Clay, *Ground Engineering* 13(6): 47–53.

Kim, N. K.; Park, J. S.; Kim S. K. 2007. Numerical Simulation of Ground Anchors, *Computers and Geotechnics* 34(6): 498–507. https://doi.org/10.1016/j.compgeo.2006.09.002

Kummerer, C. 2003. *Numerical Modelling of Displacement Grouting and Application to Case Histories.* PhD thesis. Gratz, Technische Universität Graz.

Littlejohn, G. S. 1980. Design Estimation of the Ultimate Load-Holding Capacity of Ground Anchors, *Ground Engineering* 13(8): 25–39.

Lee, S. W.; Kim, T. S.; Sim, B. K.; Kim, J. S.; Lee, I. M. 2012. Effect of Pressurized Grouting on Pullout Resistance and Group Efficiency of Compression Ground Anchor, *Canadian Geotechnical Journal* 49(8): 939–953. https://doi.org/10.1139/t2012-059

Meloun, M.; Militký, J. 2011. *Statistical Data Analysis: a Practical Guide: Complete with 1250 Exercises and Answer Key on CD*. Woodhead Publishing India. 773 p.

Mecsi, J. 1997. Some Practical and Theoretical Aspects of Grouted Soil Anchors, in *Proc. of the ICE Conference on Ground Anchors and Anchored Structures,* 20–21 March 1997, London, United Kingdom. 119–130. https://doi.org/10.1680/gaaas.26070.0012

Mišove, P. 1984. *Konštrukcia predpätých horninových kotiev a ich* únosnosť. *Doktorská práce (*PhD thesis). Bratislava, TU Bratislava (in Slovak).

Pearson, K. 1900. On the Criterion That a Given System of Deviations from the Probable in the Case of a Correlated System of Variables is Such That It Can be Reasonably Supposed to Have Arisen from Random Sampling, *Philosophical Magazine Series 5* 50(302): 157–175. https://doi.org/10.1080/14786440009463897

Sciacca, L.; Valmori, F.; Melegari, C.; Maletti, F.; Lenzi, M.; Campana, P.; Padovani, V. 2014. Theoretical and Experimental Investigation on Underwater Ground Anchors, *DFI Journal-The Journal of the Deep Foundations Institute* 5(1): 15–26. https://doi.org/10.1179/dfi.2011.002

Velič, P.; Mišove, P. 2004. *Typové skúšky dočasných horninových kotev*. Česká Třebová. Zpráva (Final Report), VUIS Zakladanie stavieb. (in Slovak)

Yurekli, K.; Kurunc. A. 2005. Testing the Residuals of an ARIMA Model on the Cekerek Stream Watershed in Turkey, *Turkish Journal of Engineering and Environmental Sciences* 29(2): 61–74.

Received 08 March 2017; accepted 06 June 2017